General Solution for Excitation by Slotted Aperture Source in Conducting Cylinder with Concentric Layering

JAMES R. WAIT, FELLOW, IEEE

Abstract —**We present a general matrix analysis for the electromagnetic fields produced by an aperture source on the inner metallic surface of a concentrically layered structure. Each layer is homogeneous and characterized by arbitrary permittivity, conductivity and magnetic permeability. The structure itself is assumed to be of infinite length, so Maxwell's equations yield separable solutions. An explicit result is given for the electric current density on the inner metallic cylindrical surface which could model the mandrel in a borehole logging tool.**

I. Introduction

In MICROWAVE logging of boreholes in applied geophysics, the objective is to launch a lateral wave into the formation that can be used as a mechanism to infer the electrical properties [1], [2]. Complications arise because a fluid layer (e.g., oil-based mud) is in the hole. Also, the region beyond the borehole boundary is invaded, so we are really dealing with a cylindrically concentric system, at least in the ideal case where the axial nonuniformities are ignored or can be separately accounted for.

We outline a general solution of the configuration with a view to providing a framework for numerical estimates for any specific parameters. We treat the problem in a general context to maintain the flexibility in later applications.

II. Statement of Problem

The general configuration is illustrated in Fig. 1. With respect to a cylindrical coordinate system (ρ, ϕ, z), the inner surface at $\rho = a_1$ is assumed to be perfectly conducting except over a finite aperture, as we discuss below. Concentric homogeneous regions are bounded by the cylindrical surfaces $\rho = a_2, a_3, \cdots, a_N$, also as shown in Fig. 1. For the nth region, for $a_n < \rho < a_{n+1}$, the conductivity, permittivity, and permeability are denoted by σ_n, ϵ_n, and μ_n, respectively. This subproblem is shown in Fig. 2.

For cylindrical configurations where the structure is invariant in the z direction, it is convenient to employ electric and magnetic Hertz vectors $\vec{i}_z U$ and $\vec{i}_z V$, respectively, where $\vec{i}_z$ is a unit vector in the z direction, and U and V are scalar functions [3]. Consequently, we are led to write

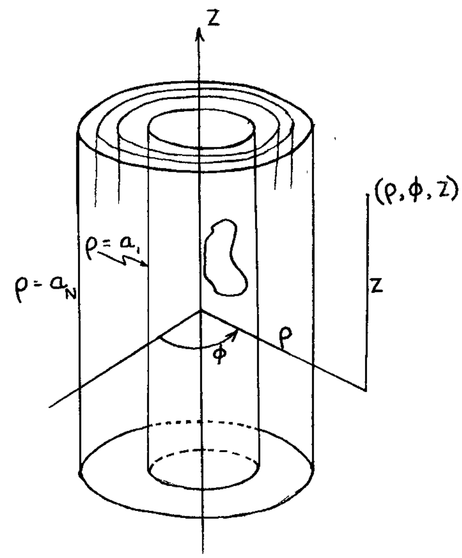

Fig. 1. General cylindrical model of concentrically layered cylinder with aperture on inner (metallic) surface.

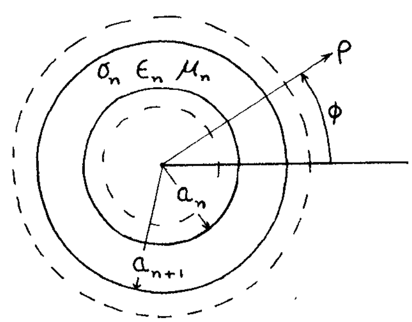

Fig. 2. End view of nth concentric region.

$$U = \int_{-\infty}^{+\infty} \left(\sum_{m=-\infty}^{+\infty} U_m(\lambda) e^{-im\phi} \right) e^{-i\lambda z} \, d\lambda \tag{1}$$

$$V = \int_{-\infty}^{+\infty} \left(\sum_{m=-\infty}^{+\infty} V_m(\lambda) e^{-im\phi} \right) e^{-i\lambda z} \, d\lambda \tag{2}$$

where $U_m(\lambda)$ and $V_m(\lambda)$ are the corresponding (double) Fourier transforms. Symbolically, we express (1) and (2) in

Manuscript received July 25, 1986; revised October 27, 1986. This work was supported in part by Schlumber-Doll facility in Ridgefield, CT.
The author is with the Electromagnetics Laboratory, ECE Department, University of Arizona, Tucson, AZ 85721.
IEEE Log Number 8612440.

0018-9480/87/0300-0321$01.00 ©1987 IEEE

the form

$$U = \Gamma U_m \tag{3}$$

and

$$V = \Gamma V_m. \tag{4}$$

The field components in the region $a_n < \rho < a_{n+1}$ are obtained by operating on the Hertz vectors; thus,

$$\vec{E} = \left(-\gamma_n^2 + \operatorname{grad}\operatorname{div}\right)\vec{i}_z U - i\mu_n\omega \operatorname{curl} \vec{i}_z V \tag{5}$$

$$\vec{H} = \left(-\gamma_n^2 + \operatorname{grad}\operatorname{div}\right)\vec{i}_z V + (\sigma_n + i\epsilon_n\omega) \operatorname{curl} \vec{i}_z U \tag{6}$$

where

$$\gamma_n = \left[i\mu_n\omega(\sigma_n + i\epsilon_n\omega)\right]^{1/2} \tag{7}$$

is the propagation constant appropriate for the adopted time factor $\exp(i\omega t)$.

Using (5) and (6), the transformed field components in the z and ϕ directions, for $a_n < \rho < a_{n+1}$, are obtained from

$$E_{zm} = -v_n^2 U_m \tag{8}$$

$$H_{zm} = -v_n^2 V_m \tag{9}$$

$$E_{\phi m} = -\frac{m\lambda}{\rho} U_m + i\mu_n\omega \frac{\partial V_m}{\partial \rho} \tag{10}$$

$$H_{\phi m} = -\frac{m\lambda}{\rho} V_m - (\sigma_n + i\epsilon_n\omega)\frac{\partial U_m}{\partial \rho} \tag{11}$$

where

$$v_n^2 = \left(\lambda^2 + \gamma_n^2\right)^{1/2}. \tag{12}$$

Here, U_m and V_m satisfy the second-order differential equation of the Bessel type

$$\left(\frac{1}{\rho}\frac{\partial}{\partial \rho}\rho\frac{\partial}{\partial \rho} - v_n^2 - \frac{m^2}{\rho^2}\right)\begin{matrix} U_m \\ V_m \end{matrix} = 0. \tag{13}$$

The appropriate general solutions of (13) are

$$U_m = A_m^n K_m(v_n\rho) + C_m^n I_m(v_n\rho) \tag{14}$$

and

$$V_m = B_m^n K_m(v_n\rho) + D_m^n I_m(v_n\rho) \tag{15}$$

where I_m and K_m are modified Bessel functions of order m and argument $v_n\rho$. The coefficients A_m^n, B_m^n, C_m^n, and D_m^n are yet to be determined.

Using (8)–(11), the transforms of the field components are

$$E_{zm}(\rho) = A_m^n\left[-v_n^2 K_m(v_n\rho)\right] + C_m^n\left[-v_n^2 I_m(v_n\rho)\right] \tag{16}$$

$$H_{zm}(\rho) = B_m^n\left[-v_n^2 K_m(v_n\rho)\right] + D_m^n\left[-v_n^2 I_m(v_n\rho)\right] \tag{17}$$

$$E_{\phi m}(\rho) = -\frac{m\lambda}{\rho}\left[A_m^n K_m(v_n\rho) + C_m^n I_m(v_n\rho)\right] + i\mu_n\omega\left[B_m^n K_m'(v_n\rho) + D_m^n I_m'(v_n\rho)\right] v_n \tag{18}$$

and

$$H_{\phi m}(\rho) = -\frac{m\lambda}{\rho}\left[B_m^n K_m(v_n\rho) + D_m^n I_m(v_n\rho)\right] - (\sigma_n + i\epsilon_n\omega)\left[A_m^n K_m'(v_n\rho) + C_m^n I_m'(v_n\rho)\right] v_n \tag{19}$$

where the primes indicate differentiation with respect to $v_n\rho$. The λ dependence of $E_{zm}(\rho)$, etc., is understood if not shown here explicitly.

III. Matrix Solution

An equivalent matrix form of (16)–(19) is

$$\bar{F}_m(\rho) = \left[P_m^n(\rho)\right]\bar{G}_m^n \tag{20}$$

where

$$\bar{F}_m(\rho) = \begin{bmatrix} E_{zm}(\rho) \\ H_{zm}(\rho) \\ E_{\phi m}(\rho) \\ H_{\phi m}(\rho) \end{bmatrix} \tag{21}$$

and

$$\bar{G}_m^n = \begin{bmatrix} A_m^n \\ B_m^n \\ C_m^n \\ D_m^n \end{bmatrix} \tag{22}$$

are column vectors and where

$$\left[P_m^n(\rho)\right] = \begin{bmatrix} -v_n^2 K\mu(v_n\rho) & 0 & -v_n^2 I_m(v_n\rho) & 0 \\ 0 & -v_n^2 K_m(v_n\rho) & 0 & -v_n^2 I_m(v_n\rho) \\ -\frac{m\lambda}{\rho}K_m(v_n\rho) & i\mu_n\omega v_n K_m'(v_n\rho) & -\frac{m\lambda}{\rho}I_m(v_n\rho) & i\mu_n\omega v_n I_m'(v_n\rho) \\ -\hat{\sigma}_n v_n K_m'(v_n\rho) & -\frac{m\lambda}{\rho}K_m(v_n\rho) & -\hat{\sigma}_n v_n I_m'(v_n\rho) & -\frac{m\lambda}{\rho}I_m(v_n\rho) \end{bmatrix} \tag{23}$$

is a 4×4 matrix with indicated ρ-dependent elements. Here, $\hat{\sigma}_n = \sigma_n + i\omega\epsilon_n$ is the complex conductivity or admittivity of the nth region bounded by $\rho = a_n$ and a_{n+1}.

We now introduce the concept of a propagation matrix by indicating how the field components at, say, $\rho = a_n$ are related to those at $\rho = a_{n+1}$. Thus, for example, from (20), we have

$$\bar{F}_m(a_{n+1}) = \left[P_m^n(a_{n+1})\right]\bar{G}_m^n. \tag{24}$$

Now, assuming that the inverse matrix exists, it follows that

$$\bar{G}_m^n = [P_m^n(a_{n+1})]^{-1}\bar{F}_m(a_{n+1}). \tag{25}$$

Then, with a further application of (20), it is evident that

$$\bar{F}_m(a_n) = [P_m^n(a_n)][P_m^n(a_{n+1})]^{-1}\bar{F}_m(a_{n+1}) \tag{26}$$

where $n = 1, 2, 2, \cdots$. Of course, (26) can be applied recursively to give

$$\bar{F}_m(a_1) = \prod_{n=1}^{N-1} [P_m^n(a_n)][P_m^n(a_{n+1})]^{-1}\bar{F}(a_N) \tag{27}$$

which relates the field column vector at $\rho = a_1$ to that at $\rho = a_N$. This result given by (27) holds quite generally provided the $N-1$ regions are homogeneous and source-free.

Now, in the context of the present problem, we can say something about the form of the fields in the semi-infinite external region. That is, for $\rho > a_N$, the coefficients C_m^N and D_m^N are zero because the function $I_m(v_n\rho)$ is not bounded as $\rho \to \infty$. Thus,

$$\bar{F}_m(a_N) = \begin{bmatrix} -v_N^2 K_m(v_N a_N) & 0 \\ 0 & -v_N^2 K_m(v_N a_N) \\ -\dfrac{m\lambda}{a_N} K_m(v_N a_N) & i\mu_N \omega v_N K_m'(v_N a_N) \\ -\hat{\sigma}_N v_N K_m'(v_N a_N) & -\dfrac{m\lambda}{a_N} K_m(v_N a_N) \end{bmatrix} \begin{bmatrix} A_m^N \\ B_m^N \end{bmatrix}. \tag{28}$$

Now this result can be inserted into (27) to obtain an equation of the form

$$\begin{bmatrix} E_{zm}(a_1) \\ H_{zm}(a_1) \\ E_{\phi m}(a_1) \\ H_{\phi m}(a_1) \end{bmatrix} = \begin{bmatrix} S_{11} & S_{21} \\ S_{12} & S_{22} \\ S_{13} & S_{23} \\ S_{14} & S_{24} \end{bmatrix} \begin{bmatrix} A_m^N \\ B_m^N \end{bmatrix} \tag{29}$$

where the S's are the elements of a 2×4 matrix. Now, in particular, we see that

$$\begin{bmatrix} E_{zm}(a_1) \\ E_{\phi m}(a_1) \end{bmatrix} = \begin{bmatrix} S_{11} & S_{21} \\ S_{13} & S_{23} \end{bmatrix} \begin{bmatrix} A_m^N \\ B_m^N \end{bmatrix} \tag{30}$$

and then

$$\begin{bmatrix} A_m^N \\ B_m^N \end{bmatrix} = \begin{bmatrix} S_{11} & S_{21} \\ S_{13} & S_{23} \end{bmatrix}^{-1} \begin{bmatrix} E_{zm}(a_1) \\ E_{\phi m}(a_1) \end{bmatrix}. \tag{31}$$

Equation (31) is a relation connecting the Fourier coefficients $A_m^N(\lambda)$ and $B_m^N(\lambda)$ for the external fields in terms of the Fourier coefficients $E_{zm}(a_1, \lambda)$ and $E_{\phi m}(a_1, \lambda)$ for the aperture electric field at the inner surface.

IV. Specific Excitation Models

To deal explicitly with the aperture conditions at the inner surface, we first note that the aperture electric fields can be represented in the form

$$E_z(a_1, \phi, z) = \Gamma E_{zm}(a_1, \lambda) \tag{32}$$

and

$$E_\phi(a_1, \phi, z) = \Gamma E_{\phi m}(a_1, \lambda) \tag{33}$$

where Γ is the double Fourier transform operator defined in accordance with (3) and (4). Now, in our statement of the problem, we specify the aperture fields, so the desired transforms are obtained from the inverse operations indicated symbolically by

$$E_{zm}(a_1, \lambda) = \Gamma^{-1}E_z(a_1, \lambda, z) \tag{34}$$

and

$$E_{\phi m}(a_1, \lambda) = \Gamma^{-1}E_\phi(a_1, \lambda, z). \tag{35}$$

For example, to be explicit,

$$E_{zm}(a_1, \lambda) = \frac{1}{(2\pi)^2}\int_{-\infty}^{+\infty}\left[\int_0^{2\pi} E_z(a_1, \phi, z) e^{+im\phi}\, d\phi\right] e^{+i\lambda z}\, dz. \tag{36}$$

A case of some interest is when the aperture is in the form of a think circumferential slot bounded by $-\phi_0 < \phi < \phi_0$ and $z_0 - d < z < z_0 + d$ (see Fig. 3). Within the slot, we will assume the vertical field has the form

$$E_z(a_1, \phi, z) = \frac{V_0}{2d}\cos\left(\frac{\pi\phi}{2\phi_0}\right) \tag{37}$$

and is zero *outside*. Here, the "voltage" at the center of the slot is denoted by V_0 while it is to vanish at the ends of the slot (i.e., at $\phi = \pm\phi_0$). Now we see that (36) is reduced as follows

$$\begin{aligned} E_{zm}(a_1, \lambda) &= \frac{V_0}{8\pi^2 d}\int_{z_0-d}^{z_0+d}\left[\int_{-\phi_0}^{\phi_0}\cos\left(\frac{\pi\phi}{2\phi_0}\right) e^{+im\phi}\, d\phi\right] e^{+i\lambda z}\, dz \\ &= \frac{V_0}{4\pi^2}\cos(m\phi_0)\frac{(\pi/\phi_0)}{\left(\dfrac{\pi}{2\phi_0}\right)^2 - m^2}\,\frac{\sin(\lambda d)}{\lambda d} e^{+i\lambda z_0} \\ &= \frac{V_0}{4\pi^2}\phi_0\frac{\sin\lambda d}{\lambda d} e^{+i\lambda z_0} \qquad \text{for } m^2 \neq \left(\frac{\pi}{2\phi_0}\right)^2. \end{aligned} \tag{38}$$

Here, we note that, for d sufficiently small, the factor $(\sin\lambda d)/\lambda d$ can be replaced by 1. Also, in the case of the thin circumferential slot, the E_ϕ component of the field

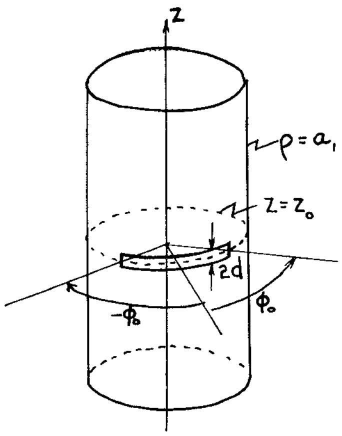

Fig. 3. Circumferentially slotted aperture.

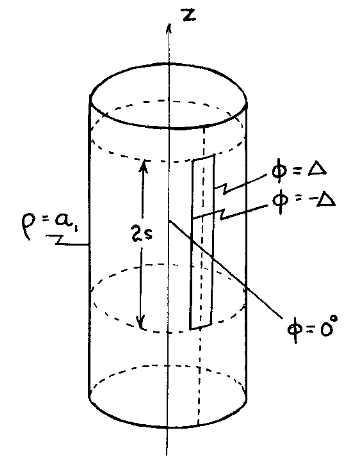

Fig. 4. Axially slotted aperture.

can be neglected. Thus, in the example just considered, $E_{\phi m}(a_1, \lambda)$ is effectively zero.

Another particular source model is a narrow axial slot bounded by $-\Delta < \phi < \Delta$ and $-s < z < s$ (see Fig. 4). A reasonable assumption for the circumferential field within the slot is

$$E_\phi(a, \phi, z) = \frac{V_1}{2a_1\Delta} f(z) \tag{39}$$

where $f(z)$ is the distribution of the aperture field in the axial direction. We choose the normalization $f(0) = 1$ so that V_1 is then the "voltage" at the center of the slot. Now (35) has the explicit form

$$E_{\phi m}(a_1, \lambda) = \frac{V_1}{8\pi^2 a_1 \Delta} \int_{-s}^{s} \left[\int_{-\Delta}^{\Delta} e^{+im\phi} \, d\phi \right] f(z) e^{+i\lambda z} \, dz$$
$$= \frac{V_1}{4\pi^2 a_1} \frac{\sin m\Delta}{m\Delta} \int_{-s}^{s} f(z) e^{+i\lambda z} \, dz. \tag{40}$$

Now, if Δ is sufficiently small, $(\sin m\Delta)/(m\Delta)$ can be replaced by 1. Furthermore, in the case of a thin axial slot, $E_z(a_1, \phi)$ within the aperture is negligible so that, in this case, $E_{zm}(a_1, \lambda)$ is effectively zero.

We have only shown two specific examples of slot geometry. Of course, there are many other possibilities. For some purposes, we may wish to employ an array of slot apertures. If we can neglect the mutual coupling, the analysis is very straightforward, being just a matter of integration over the assumed aperture fields.

V. Induced Surface Current

For the borehole applications, we are interested primarily in detecting the induced surface current density on the inner metallic boundary (e.g., the mandrel). Thus, the relevant quantities are $H_z(a_1, \phi, z)$ and $H_\phi(a_1, \phi, z)$, which have dimensions of A/m. Thus, we need to evaluate

$$\begin{bmatrix} H_z(a_1, \phi, z) \\ H_\phi(a_1, \phi, z) \end{bmatrix} = \int_{-\infty}^{+\infty} \sum_{m=-\infty}^{+\infty} \begin{bmatrix} H_{zm}(a_1, \lambda) \\ H_{\phi m}(a_1, \lambda) \end{bmatrix} e^{-im\phi} e^{-i\lambda z} \, d\lambda \tag{41}$$

where, in accordance with (29) and (30),

$$\begin{bmatrix} H_{zm}(a_1, \lambda) \\ H_{\phi m}(a_1, \lambda) \end{bmatrix} = \begin{bmatrix} S_{12} & S_{22} \\ S_{14} & S_{24} \end{bmatrix} \begin{bmatrix} S_{11} & S_{21} \\ S_{13} & S_{23} \end{bmatrix}^{-1} \begin{bmatrix} E_{zm}(a_1, \lambda) \\ E_{\phi m}(a_1, \lambda) \end{bmatrix}. \tag{42}$$

The elements in this key matrix operation are obtained from (27). To be explicit,

$$\begin{bmatrix} S_{11} & S_{21} \\ S_{12} & S_{22} \\ S_{13} & S_{23} \\ S_{14} & S_{24} \end{bmatrix} = \prod_{n=1}^{N-1} [P_m^n(a_n)][P_m^n(a_{n+1})]^{-1} \begin{bmatrix} - & - \\ - & - \\ - & - \\ - & - \end{bmatrix} \tag{43}$$

where the latter 2×4 matrix is given in (28)

VI. Concluding Remarks

While the general evaluation of the field integrals is not a trivial task, certain physical concepts are evident from the preceding analysis. For example, in dealing with (41), we must cope with an integral of the form

$$F_m(z) = \int_{-\infty}^{+\infty} f_m(\lambda) e^{-i\lambda z} \, d\lambda \tag{44}$$

where the transform $f_m(\lambda)$ is known as a function of λ for each integer m. The integration contour is along the entire real axis of λ, as indicated in the discussion below. Now, clearly we need to evaluate the inverse transform $F_m(z)$ as a function of z. The task is quite similar to a similar class of problems encountered in wave transmission in planar and spherical geometries such as the earth–ionosphere waveguide [4].

In the ideal case here, we are attempting to launch a wave into the outer formation. Such a wave propagates parallel to the borehole axis. This contribution to the total field is usually called the lateral wave. It is exploited in recent developments in microwave logging [5]–[7]. Unfortunately, the complexity of the borehole environment greatly complicates the quantitative interpretation. In fact, additional transmission modes may compete with the desired lateral wave. The physical picture of the propagation phenomena is shown in Fig. 5, which is highly oversim-

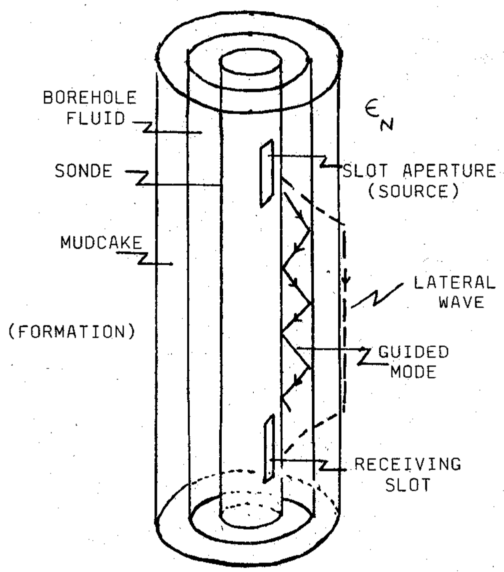

Fig. 5. Physical picture of propagation modes for transmission between apertures. The receiving slot here is to detect the induced surface current density.

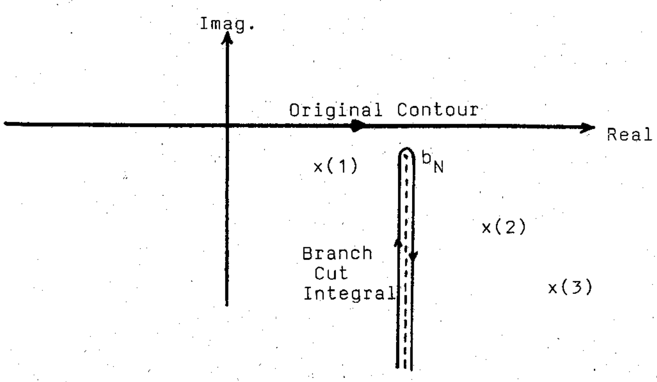

Fig. 6. The complex λ plane showing the original and deformed contours and the location of the pole and branch cut singularities.

plified. The lateral wave is shown as a ray being critically reflected at the outer cylindrical interface. On the other hand, any number of waveguide modes may be transmitted within the inner concentric layers; only one is depicted in Fig. 5.

If we return to our integral representation given by (44), we see that the original contour, along the real axis, leads to a difficult convergence problem because of the highly oscillatory nature of the integrand. However, we may deform the contour to encircle the pole singularities denoted by $x(1)$, $x(2)$, $x(3), \cdots$, as indicated in Fig. 6. The deformed contour, of course, must also enclose or be wrapped around the branch line drawn from the branch point at $\lambda = b_N = -i\gamma_N$. This standard procedure is also shown in Fig. 6. Actually, for the present problem, there are no other branch points because it can be shown that the integrand in (44) is an even function of v_n for $n = 1, 2, 3, \cdots, N-1$. This point was nicely demonstrated by Chew [8] in a related study. In fact, it is a quite general property of wave transmission in stratified media. The branch points associated with the continuous spectra are only present in open regions or in penetrable core regions, such as in a dielectric rod. The bounded regions (i.e., the layers) possess only discrete spectra which correspond to the waveguide modes.

The general formulation here can be specialized to a geometry involving only a single layer or coating. We then recover earlier formulations which have been applied to radiation from slotted cylinder antennas [9]. In such cases, we can deal with the integrals using a saddle-point method which really is an alternative way to cope with the branch cut contribution. However, if we are interested in the electromagnetic field at any distance from the cylinder axis, attention must be paid to the role of the pole singularities which represent the trapped waveguide modes on the structure. We will deal with these matters in a sequel to this paper.

References

[1] R. Freedman and J. P. Vogiatzis, "Theory of microwave dielectric logging using the electromagnetic wave propagation method," *Geophysics*, vol. 44, no. 5, pp. 969–986, 1979.
[2] W. C. Chew and S. C. Gianzero, "Theoretical investigations of the electromagnetic wave propagation tool," *IEEE Trans. Geosci. Remote Sensing*, vol. GE-19, no. 1, pp. 1–7, 1981.
[3] J. R. Wait, *Electromagnetic Wave Theory*. New York: Harper & Row, 1985, ch. 6.
[4] J. R. Wait, *Wave Propagation Theory*. Elmsford, NY: Pergamon, 1981, ch. 14.
[5] R. P. Wharton, G. A. Hazen, R. N. Rau, and D. L. Best, "Electromagnetic logging: Advances in technique and interpretation," in *Proc. Society of Petroleum Engineers of AIME*, 1980, paper no. 9267, pp. 1–12.
[6] R. P. Singh, "Propagation time of microwave signals for some Indian rock samples," *Gerlands Beitr. Geophysik*, vol. 92, no. 6, pp. 493–497, 1983.
[7] L. C. Shen, "Problems in dielectric constant logging and possible routes to their solution," *The Log Analyst*, vol. 26, no. 5, pp. 14–25, 1985.
[8] W. C. Chew, "The singularities of a Fourier type integral in a multi-layer cylindrical problem," *IEEE Trans. Antennas Propagat.*, vol. AP-31, pp. 653–655, 1983.
[9] J. R. Wait, Electromagnetic Radiation from Cylindrical Structures. Elmsford, NY: Pergamon, 1959 (reprinted 1985).

James R. Wait (SM'56–F'62) received the B.A.Sc., M.A.Sc., and Ph.D. degrees from the University of Toronto. From 1955 to 1980, he was a member of the scientific community in Boulder, CO. His positions included Senior Scientist in NOAA, Professor Adjoint in Electrical Engineering at the University of Colorado, Consultant to the Institute of Telecommunications, and a (founding) Fellow of the Cooperative Institute of Environmental Sciences. In 1980, he became Professor of Electrical Engineering and Geosciences at the University of Arizona in Tucson.

Dr. Wait has received numerous awards for his research in electromagnetics and electrical geophysics, among them the Balth van der Pol Gold Medal, presented by URSI in Helsinki in 1978, the IEEE Centennial Medal in 1984, and the IEEE Geoscience and Remote Sensing Achievement Award in 1985. He is a member of the (US) National Academy of Engineering.